Coherent Structures in Monolayers of Swimming Particles

Takuji Ishikawa[1] and T. J. Pedley[2]

[1]Department of Bioengineering and Robotics, Tohoku University, Sendai 980-8579, Japan
[2]Department of Applied Mathematics and Theoretical Physics, University of Cambridge, Cambridge CB3 0WA, United Kingdom

(Received 10 July 2007; published 27 February 2008)

We report various types of coherent structures in suspensions of spherical particles swimming in a monolayer. We solve the fluid dynamics precisely from far-field hydrodynamic interactions to lubrication between two near-contact surfaces. The simulation results clearly illustrate that coherent structures, such as aggregation, mesoscale spatiotemporal motion, and band formation, can be generated by purely hydrodynamic interactions.

DOI: 10.1103/PhysRevLett.100.088103 PACS numbers: 47.63.−b

Systems of swimming organisms exhibit an interesting variety of collective behavior such as clustering and migration; examples include schools of fish and coherent structures of swimming bacteria. In the case of swimming microorganisms, the collective motions may be generated passively as a result of hydrodynamic interactions. Ishikawa and Hota [1] showed for interacting *Paramecium caudatum* cells that most swimming cell interactions are hydrodynamic. Even when the collective motions are generated passively, it is still important to discuss whether the collective motions are biologically and evolutionarily favorable or not in various conditions. Recently, there has been increasing interest in the collective dynamics of swimming bacteria, because some species of bacteria show spatiotemporally coherent structures [2,3]. It is also reported experimentally that self-diffusion in such suspensions is considerably enhanced by the coherent structures [4]. Moreover, in older studies using magnetotactic bacteria, it was observed that thousands of cells form a stable band perpendicular to the swimming direction [5].

In this work we report various types of coherent structures that arise from computations of monolayer suspensions of swimming particles in order to improve our understanding of the experimental observations. We employ a simple model of swimming microorganisms; however, we solve the fluid dynamics precisely from far-field hydrodynamic interactions to lubrication between two near-contact surfaces. Though the number of particles we can deal with in the system is limited by this precise treatment, we can see the effect of near-field fluid dynamics on the collective motions. We also allow for bottom-heaviness of the microorganisms, leading to external gravitational torques when the cells are not oriented vertically [6]. The simulation results clearly illustrate that various coherent structures, such as aggregation, mesoscale spatiotemporal motion, and band formation, can be generated by purely hydrodynamic interactions.

In previous studies, the collective motions of locomotive particles, such as aggregations, coherent motions, and ordered motions, have been modeled in various ways. In Vicsek's model [7], locomotive particles are driven at a constant speed and they are oriented parallel to the average direction of the surrounding particles with some random perturbation added. Ramaswamy and co-workers [8,9] constructed hydrodynamic equations for suspensions of self-propelled particles by adding a distribution of force dipoles caused by the locomotive particles. In Hernandes-Ortiz's model [10], the swimming motion of bacterium was modeled by two point forces, corresponding to the flagellum force and to the drag force. Most recently, Saintillan and Shelley [11] used slender-body theory to investigate orientational order in suspensions of self-locomoting rods. Although the results obtained from these former studies are suggestive and consistent with experimental observations, they did not treat near-field fluid dynamics precisely. Our former studies [1,12] revealed, however, that near-field fluid dynamics play an important role in the orientational change of microorganisms. Thus, in this Letter, we solve both far- and near-field fluid dynamics precisely and perform Stokesian-dynamics simulation of swimming particles for the first time.

A swimming microorganism is modeled as a squirming sphere with prescribed tangential surface velocity, which will be referred to as a squirmer [12,13]. The squirmer is assumed to be neutrally buoyant, but the center of gravity of the spherical cell may not coincide with its geometric center (bottom-heaviness), as shown in Fig. 1. We assume that the flow field around the microorganisms is Stokes flow, and Brownian motion is not taken into account. The surface of the spherical squirmer is assumed to move purely tangentially and these tangential motions are assumed to be axisymmetric, time independent, and invariant during the interactions. The surface velocity of a squirmer $\mathbf{u}_s$ was analyzed by Blake [14] and is given by

$$\mathbf{u}_s = \sum_{n=1}^{2} \frac{2}{n(n+1)} B_n \left(\frac{\mathbf{e}\cdot\mathbf{r}}{r}\frac{\mathbf{r}}{r} - \mathbf{e} \right) P_n'(\mathbf{e}\cdot\mathbf{r}/r), \qquad (1)$$

where $\mathbf{e}$ is the orientation vector of the squirmer, B_n is the nth mode of the surface squirming velocity, P_n is the nth Legendre polynomial, $\mathbf{r}$ is the position vector, and $r = |\mathbf{r}|$.

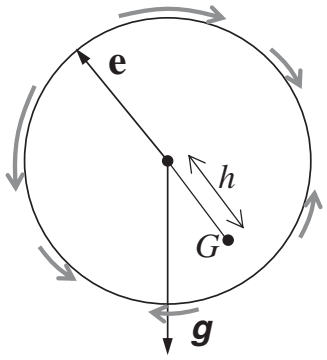

FIG. 1. A sketch of the arrangement of a bottom-heavy squirmer. Gravity acts in the $\boldsymbol{g}$ direction, while the squirmer has orientation vector $\mathbf{e}$. G is the center of gravity. Gray arrows schematically show the squirming velocity on the surface.

The swimming speed of a solitary squirmer is $2B_1/3$. We denote by β the ratio of second mode squirming to first mode squirming, i.e., $\beta = B_2/B_1$. It should be noted that B_2, and hence β, can have either sign. A squirmer with positive β is a puller, analogous to a microorganism for which the thrust-generating apparatus is in front of the body, as for biflagellate algae such as *Chlamydomonas*, whereas a squirmer with negative β is a pusher, i.e., the thrust is generated behind the body, as for bacteria or spermatozoa. We show the results for $-5 \le \beta \le 5$ in this paper.

The Stokesian-dynamics method [15] is employed in order to simulate dynamic motions of squirmers in an infinite suspension. The hydrodynamic interactions among an infinite suspension of particles are computed by the Ewald summation technique. By exploiting the Stokesian-dynamics method [15], the force $\mathbf{F}$, torque $\mathbf{L}$, and stresslet $\mathbf{S}$ balances of squirmers are given by

$$\begin{pmatrix} \mathbf{F} \\ \mathbf{L} \\ \mathbf{S} \end{pmatrix} = [\mathbf{R}^{\mathrm{far}} - \mathbf{R}^{\mathrm{far}}_{2B} + \mathbf{R}^{\mathrm{near}}_{2B}] \begin{pmatrix} \mathbf{U} - \langle \mathbf{u} \rangle \\ \boldsymbol{\Omega} - \langle \boldsymbol{\omega} \rangle \\ -\langle \mathbf{E} \rangle \end{pmatrix} + [\mathbf{R}^{\mathrm{far}} - \mathbf{R}^{\mathrm{far}}_{2B}] \begin{pmatrix} -\frac{2}{3} B_1 \mathbf{e} + \mathbf{Q}_{\mathrm{sq}} \\ 0 \\ -\frac{1}{5} B_2 (3\mathbf{ee} - \mathbf{I}) \end{pmatrix} + \begin{pmatrix} \mathbf{F}^{\mathrm{near}}_{\mathrm{sq}} \\ \mathbf{L}^{\mathrm{near}}_{\mathrm{sq}} \\ \mathbf{S}^{\mathrm{near}}_{\mathrm{sq}} \end{pmatrix}, \quad (2)$$

where $\mathbf{R}$ is the resistance matrix, $\mathbf{U}$ and $\boldsymbol{\Omega}$ are the translational and rotational velocities of a squirmer, $\langle \mathbf{u} \rangle$ and $\langle \omega \rangle$ are the translational and rotational velocity of the bulk suspension, and $\langle \mathbf{E} \rangle$ is the rate of strain tensor of the bulk suspension. $\mathbf{Q}$ is the irreducible quadrupole providing additional accuracy, which is approximated by its mean-field value (cf. [15]). Index far or near indicates far- or near-field interaction, and $2B$ or sq indicates interaction between two inert spheres or two squirmers, respectively. A simplified version of this method was reported in [16], and the derivation of Eq. (2) is explained fully in [17].

We calculate interacting squirmers' motion in a fluid otherwise at rest swimming in a monolayer, in which all squirmers' centers and orientation vectors are on the same x-y plane though the flow field is fully three-dimensional. Restriction to a monolayer configuration is a very strong limitation. But some of the aforementioned experimental observations are also restricted in some way; for instance, the collective motions were restricted by a plane wall in [2], and the motions are restricted to a 2D film in [3,4]. Another advantage of the monolayer configuration is that one can deal with a larger computational domain than a fully three-dimensional configuration. Since the number of particles we can include in the system is limited due to the precise treatment of hydrodynamic interactions, this advantage is crucial. In order to treat the monolayer configuration we will follow the method employed by Dratler and Schowalter [18]. The computational region is a square of side H, and a suspension of infinite extent is modeled with periodic boundary conditions in the x and y directions. The monolayer is periodically replicated also in the z direction with $10H$ intervals, in order to maintain the positive-definite mobility matrix. We have considered three different cases, with a particle number $N = 100$ for $c_a = 0.1$, 144 for $c_a = 0.3$, and 196 for $c_a = 0.5$, where c_a is the areal fraction of particles in the monolayer.

Movement of non-bottom-heavy squirmers with $\beta = 5$ is computed for random initial positions and orientations. The distributions of squirmers in one realization for $c_a = 0.1$ and 0.5 are shown in Fig. 2, where the velocity vectors of squirmers are shown as arrows on spheres. It is found that clusters are formed in these cases, and some squirmers in the cluster move together and generate collective motions. In order to clarify the scale of the collective motions, we calculate the velocity correlation among particles, $I_U(r)$, as shown in Fig. 3 for the three cases $c_a = 0.1$, 0.3, 0.5. I_U is positive when $r < 6$, showing that neighboring squirmers tend to swim together in a similar direction. The results show anticorrelation when $10 < r$, so squirmers more than 10 radii apart swim in opposite directions on average; this defines the typical scale of the coherent structures. We should note that the scale of the coherent structures for $c_a = 0.5$ increases slightly as the domain size increases, though it does not affect the coherent structures qualitatively. In Dombrowski's experiment [2] using rod-shaped bacteria of size 4×0.7 μm, they observed anticorrelation when 50 $\mu\mathrm{m} < r$. In Mendelson's experiment [3] using the same bacteria, they observed whirls, each approximately 1000 $\mu\mathrm{m}^2$. The whirl structure appearing in the present study is smaller than these experiments. However, the collective motions observed in the present study occur randomly in time and in space, and these tendencies show good qualitative agreement with previous experiments.

Figure 4 shows the effect of β on the length of the orientation vector averaged over all squirmers, referred to as $\mathbf{e}_{\mathrm{av}}$. $\mathbf{e}_{\mathrm{av}}$ can be large when $\beta = \pm 1$, which indicates that

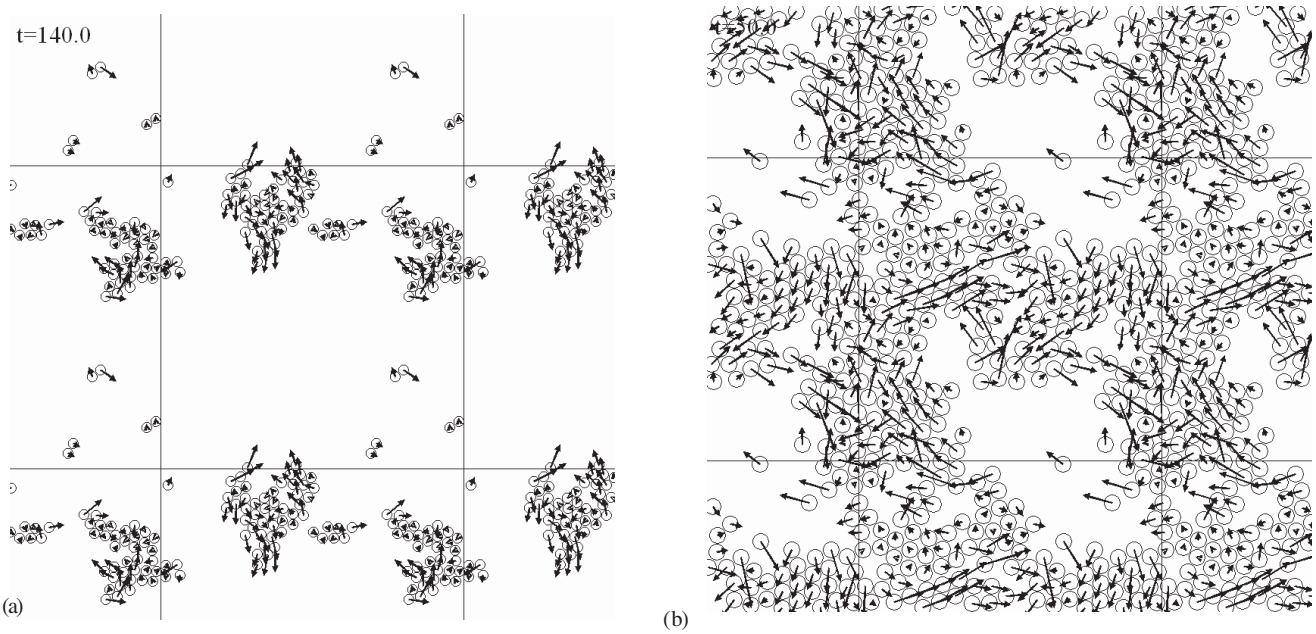

FIG. 2. Velocity vectors relative to the average squirmer velocity ($\beta = 5$). The computational cell is located at the center as indicated by the solid lines.

squirmers tend to swim in a similar direction. Though we did not observe a significant effect of the domain size on the value of $\mathbf{e}_{\mathrm{av}}$, an effect may appear in very large domains, due to the possible instability of the ordered motion. $\mathbf{e}_{\mathrm{av}}$ is small and fluctuates frequently when $\beta = \pm 5$, which indicates that squirmers orientate chaotically and tend to change their orientation frequently. (The results for $\beta = -5$ are omitted from Fig. 4, because they considerably overlap those for $\beta = 5$.) Random perturbation in the squirmer orientation increases as $|\beta|$ is increased, because hydrodynamic interactions between squirmers become stronger (cf. [19]).

Bottom-heavy squirmers tend to swim upwards. The distribution and velocity vectors of squirmers, relative to the average velocity, are shown in Fig. 5 [$(2\pi\rho gah)/(\mu B_1) = 100$ and $\beta = 1$, where ρ is the density, a is the radius, μ is the viscosity, and h is the distance between the geometric center and the center of gravity]. Though initially squirmers are placed randomly, they tend to form a large band perpendicular to the gravitational direction in this case. We observed that squirmers on the top side of the band tend to swim away from the tip, and squirmers on the bottom side tend to swim toward the tip, which generates a pair of large rotational motions. The band formation appearing in this study is similar to the band formation observed in swim-

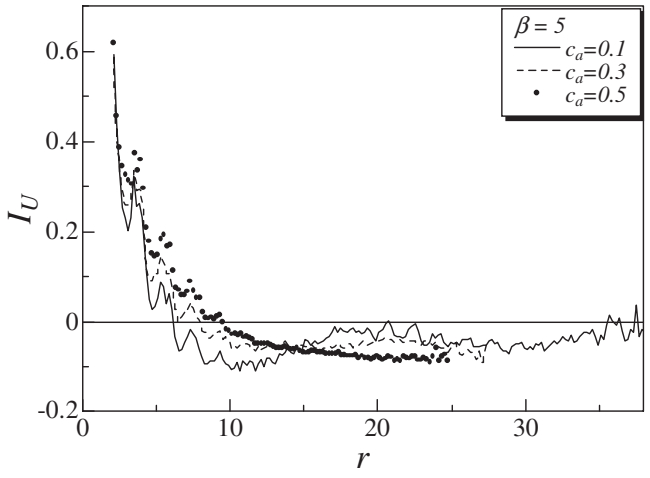

FIG. 3. Correlation of the velocity of squirmers with $\beta = 5$ under $c_a = 0.1$, 0.3, and 0.5 conditions.

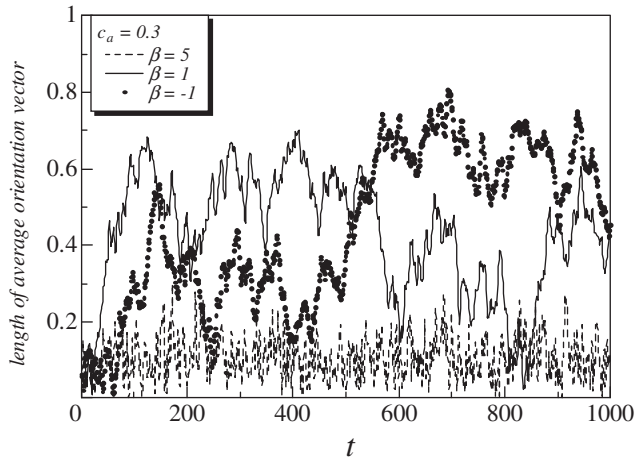

FIG. 4. Effect of β on the time change of the length of squirmer averaged orientation vectors for $c = 0.3$.

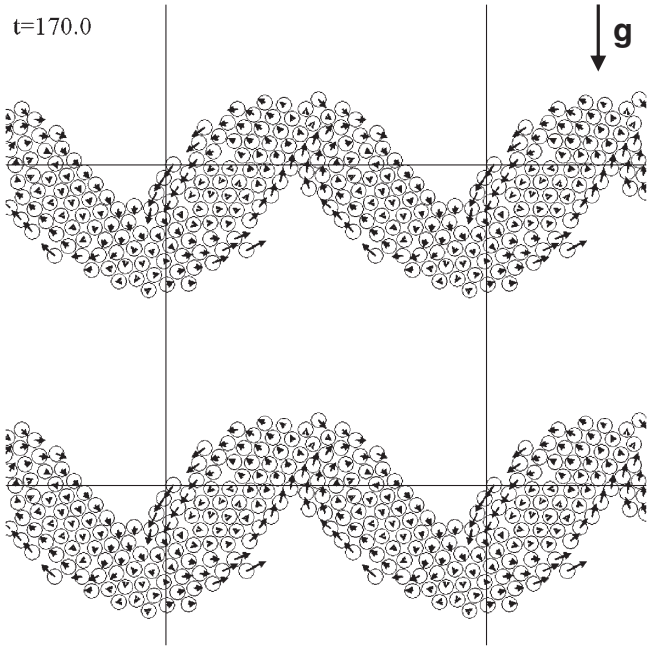

FIG. 5. Velocity vectors of bottom-heavy squirmers with $\beta = 1$, relative to the average squirmer velocity ($c_a = 0.3$).

ming magnetotactic bacteria [5]. There are two kinds of dipole acting on a magnetotactic bacterium: the magnetic dipole due to permanent magnetic particles in a cell and the hydrodynamic force dipole due to the swimming motion of a cell. Carlile *et al.* [20] speculated that band formation resulted from the magnetic interaction. However, Guell *et al.* [21] suspected that it resulted from the hydrodynamic interaction. In the present study, we observed the band formation only when β is positive (β for bacteria is negative). Although a squirmer models only the leading-order flow singularity (stresslet) of a bacterium, our results appear to conflict with Guell's hypothesis.

We have shown various types of coherent structures in suspensions of swimming particles, such as aggregation, mesoscale spatiotemporal motion, and band formation. The simulation results clearly illustrate that they can be generated by purely hydrodynamic interactions. It is worth adding that fully three-dimensional simulations, not restricted to a monolayer, have also been performed [17,19] and do not show such dramatic coherent structures: 2D and 3D suspensions are quite different.

The authors are grateful for helpful discussions with J. T. Locsei in DAMTP, University of Cambridge. This work is partly supported by Grant-in-Aid for Young Scientists (A) by the JSPS No. 19686016.

[1] T. Ishikawa and M. Hota, J. Exp. Biol. **209**, 4452 (2006).
[2] C. Dombrowski, L. Cisneros, S. Chatkaew, R. E. Goldstein, and J. O. Kessler, Phys. Rev. Lett. **93**, 098103 (2004).
[3] N. H. Mendelson, A. Bourque, K. Wilkening, K. R. Anderson, and J. C. Watkins, J. Bacteriol. **181**, 600 (1999).
[4] Xiao-Lun Wu and A. Libchaber, Phys. Rev. Lett. **84**, 3017 (2000).
[5] A. M. Spormann, FEMS Microbiol. Ecol. **45**, 37 (1987).
[6] J. O. Kessler, Progress in Phycological Research **4**, 257 (1986).
[7] T. Vicsek, A. Czirók, E. Ben-Jacob, I. Cohen, and O. Shochet, Phys. Rev. Lett. **75**, 1226 (1995).
[8] R. A. Simha and S. Ramaswamy, Phys. Rev. Lett. **89**, 058101 (2002).
[9] Y. Hatwalne, S. Ramaswamy, M. Rao, and R. A. Simha, Phys. Rev. Lett. **92**, 118101 (2004).
[10] J. P. Hernandes-Ortiz, C. G. Stoltz, and M. D. Graham, Phys. Rev. Lett. **95**, 204501 (2005).
[11] D. Saintillan and M. J. Shelley, Phys. Rev. Lett. **99**, 058102 (2007).
[12] T. Ishikawa, M. P. Simmonds, and T. J. Pedley, J. Fluid Mech. **568**, 119 (2006).
[13] M. J. Lighthill, Commun. Pure Appl. Math. **5**, 109 (1952).
[14] J. R. Blake, J. Fluid Mech. **46**, 199 (1971).
[15] J. F. Brady, R. J. Phillips, J. C. Lester, and G. Bossis, J. Fluid Mech. **195**, 257 (1988).
[16] T. Ishikawa and T. J. Pedley, J. Fluid Mech. **588**, 399 (2007).
[17] T. Ishikawa, J. T. Locsei, and T. J. Pedley, J. Fluid Mech. (to be published).
[18] D. I. Dratler and W. R. Schowalter, J. Fluid Mech. **325**, 53 (1996).
[19] T. Ishikawa and T. J. Pedley, J. Fluid Mech. **588**, 437 (2007).
[20] M. Carlile, A. W. L. Dudeney, B. K. Hebenstreit, and R. H. Heerema, J. Magn. Magn. Mater. **67**, 291 (1987).
[21] D. C. Guell, H. Brenner, R. B. Frankel, and H. Hartman, J. Theor. Biol. **135**, 525 (1988).